Acta Crystallographica Section F
Structural Biology and Crystallization Communications
ISSN 1744-3091

Crystallization of Spätzle, a cystine-knot protein involved in embryonic development and innate immunity in *Drosophila melanogaster*

Anita Hoffmann,[a] Piotr Neumann,[a] Angelika Schierhorn[b] and Milton T. Stubbs[a,c]*

[a]Institut für Biochemie und Biotechnologie, Martin-Luther-Universität Halle-Wittenberg, Abteilung Physikalische Biotechnologie, Kurt-Mothes-Strasse 3, 06120 Halle (Saale), Germany, [b]Max-Planck-Institut für Proteinfaltung, Abteilung Massenspektrometrie, Kurt-Mothes-Strasse 3, 06120 Halle (Saale), Germany, and [c]Mitteldeutsches Zentrum für Struktur und Dynamik der Proteine (MZP), Martin-Luther-Universität Halle-Wittenberg, Germany

Correspondence e-mail: stubbs@biochemtech.uni-halle.de

Received 13 March 2008
Accepted 21 June 2008

The Spätzle protein is involved in both the definition of the dorsal–ventral axis during embryonic development and in the adult innate immune response. The disulfide-linked dimeric cystine-knot protein has been expressed as a proprotein in inclusion bodies in *Escherichia coli* and refolded *in vitro* by rapid dilution. Initial orthorhombic crystals that diffracted to 7 Å resolution were obtained after three months by the sitting-drop vapour-diffusion method. Optimization of the crystallization conditions resulted in orthorhombic crystals (space group $P2_12_12_1$, with unit-cell parameters $a = 53.0$, $b = 59.2$, $c = 62.5$ Å) that diffracted to 2.8 Å resolution in-house. The small volume of the asymmetric unit indicated that it was not possible for the crystals to contain the complete pro-Spätzle dimer. Mass spectrometry, N-terminal sequencing and Western-blot analysis revealed that the crystals contained the C-terminal disulfide-linked cystine-knot dimer. Comparison of various crystallization experiments indicated that degradation of the N-terminal prodomain was dependent on the buffer conditions.

1. Introduction

The Spätzle protein is the precursor of a nerve-growth-factor-like ligand in *Drosophila melanogaster* (Stein *et al.*, 1991). It plays a role in definition of the dorsal–ventral axis of the *Drosophila* embryo (Schneider *et al.*, 1994) and acts in the initiation of immune responses to fungal and bacterial infection in adult flies (Hoffmann, 2003). An extracellular proteolytic cascade results in activation of Spätzle, which in turn leads to signalling by the transmembrane receptor Toll. In the developmental pathway, the trypsin-like serine protease Easter cleaves Spätzle to generate a 12 kDa C-terminal fragment. The recently discovered Spätzle-processing enzyme (SPE; Jang *et al.*, 2006) activates Spätzle in the infectional pathway *via* the same cleavage, initiating an immune response that leads to drosomycin generation. Dimers of the C-terminal fragment have been found *in vivo* (DeLotto & DeLotto, 1998) as have dimers of the proprotein *in vitro* (Hoffmann *et al.*, 2008; Weber *et al.*, 2005, 2007). Binding of activated Spätzle to Toll leads to receptor dimerization and autophosphorylation of the cytosolic Toll/interleukin-1 receptor (TIR) domains (Weber *et al.*, 2003, 2005). The receptor shares significant sequence similarity to the vertebrate interleukin-1 receptor (Schneider *et al.*, 1994) as well as to mammalian Toll-like receptors (Jin *et al.*, 2007).

The spacing of the cysteine residues and the sequence homology of the C-terminal 106 amino acids of Spätzle to coagulogen (Bergner *et al.*, 1996) and mature human nerve growth factor (NGF; McDonald *et al.*, 1991) suggest a cystine-knot motif: two disulfide bridges that form a ring through which a third disulfide bridge is threaded (Mizuguchi *et al.*, 1998). Here, we describe the crystallization of the recombinantly expressed and *in vitro* folded Spätzle C-terminal domain derived from pro-Spätzle isoform Spz11.7.

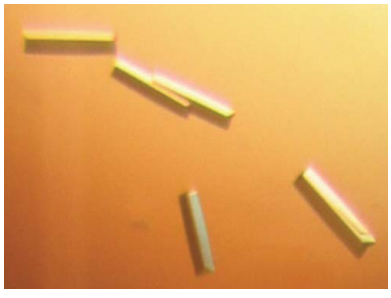

Table 1
Data-collection and processing statistics.

Values in parentheses are for the highest resolution shell.

Space group	$P2_12_12_1$
Unit-cell parameters	
a (Å)	53.0
b (Å)	59.2
c (Å)	62.5
Wavelength (Å)	1.5418
Mosaicity (°)	0.5
Resolution range (Å)	30.0–2.8 (2.9–2.8)
Total no. of reflections	84797 (5203)
Unique reflections	8348 (500)
Redundancy	16.3 (16.7)
Completeness (%)	99.8 (100.0)
$I/\sigma(I)$	24.6 (4.5)
$R_{\rm merge}$† (%)	9.8 (75.9)
Wilson *B* factor (Å^2)	54.7
Molecules per ASU	2
Matthews coefficient (Å^3 Da^{-1})	2.23
Solvent content (%)	45

† $R_{\rm merge} = \sum_{hkl}\sum_i |I_i(hkl) - \langle I(hkl)\rangle| / \sum_{hkl}\sum_i I_i(hkl)$.

2. Materials and methods

2.1. Protein purification

The expression of C-terminally His_6-tagged pro-Spätzle isoform Spz11.7 as insoluble inclusion bodies with subsequent solubilization and refolding has been described elsewhere (Hoffmann *et al.*, 2008). Briefly, inclusion-body protein dissolved in 6 *M* guanidinium hydrochloride was renatured by rapid dilution (Rudolph & Lilie, 1996) into 1 *M* l-arginine, 0.1 *M* Tris–HCl, 5 m*M* EDTA pH 8.5 with an oxidized/reduced glutathione redox-shuffling system in the ratio 1 to 5 m*M*. After concentration and dialysis in 20 m*M* sodium phosphate, 20 m*M* sodium chloride pH 7.4, dimers were separated from monomers and aggregates by size-exclusion chromatography (HiLoad 26/60 Superdex 75pg, GE Healthcare). Pooled dimer fractions were concentrated to 20 mg ml^{-1} according to the optical density $OD_{280\,nm}$ using Amicon filter devices (10 000 Da molecular-weight cutoff; Millipore) and used for further crystallization trials.

2.2. Crystallization and optimization

Initial sitting-drop vapour-diffusion crystallization experiments were carried out with a variety of commercially available crystallization screens using a Cartesian Microsys NQ crystallization robot (Zinsser Analytik, Frankfurt, Germany). Crystallization in 96-well plates (CrystalQuick, Greiner) with 200 nl drops and 110 µl reservoir volumes was monitored using an OASIS LS3 imaging system (Veeco, Tucson, Arizona, USA). The first crystals appeared after three months in 50 m*M* Tris–HCl, 20% PEG 3350 pH 8.0 (Sigma–Aldrich, low ionic strength crystallization kit) at 293 K. Optimization using hanging-drop vapour diffusion (in EasyXtal plates, Qiagen) involved mixing the contents of an additive screen (Hampton Research) with the crystallization drops (1 µl protein solution + 1 µl reservoir solution) in a 1:10 ratio and equilibrating against 500 µl reservoir solution. Two additive conditions (0.1 *M* betaine monohydrate and 0.1 *M* phenol in 50 m*M* Tris–HCl, 20% PEG 3350 pH 8.0) yielded crystals that grew within three weeks.

2.3. Data collection

Crystals were mounted directly in a 100 K cryostream (XSTREAM2000; Rigaku/MSC, Japan) without any additional cryoprotection. Diffraction data were collected in-house using Cu $K\alpha$ radiation with an R-AXIS IV^{++} imaging-plate system (Rigaku/MSC, Japan) mounted on a Rigaku MM-007 rotating-anode generator. Initial crystals from the 96-well plates diffracted anisotropically to 7 Å resolution. Larger crystals obtained using betaine monohydrate from the additive screen also diffracted anisotropically, but the data could be scaled and processed to 2.8 Å resolution using *XDS* (Kabsch, 1993).

2.4. Analysis of the crystallized fragment

2.4.1. Mass spectrometry. Samples from crystallization drops with similar conditions to those containing crystals were taken for MALDI-MS (matrix-assisted laser desorption/ionization mass spectrometry) analysis. Protein bands excised from nonreducing denaturing SDS gels were washed three times with water, twice with 10 m*M* ammonium bicarbonate and finally with 10 m*M* ammonium bicarbonate in 50% acetonitrile. The gel slices were dried under a gentle stream of nitrogen, re-swollen in 20 µl 10 m*M* ammonium bicarbonate pH 8.0 and digested with trypsin (Promega, USA) overnight at 310 K. 0.5 µl of a saturated solution of α-cyano-4-hydroxycinnamic acid in acetone was deposited onto the anchor target and 1 µl of the digest was added to the matrix layer. After evaporation of the solvent, the spot was recrystallized with 1 µl ethanol:acetone:0.1% trifluoroacetic acid (6:3:1). The peptide mass-fingerprint spectra were recorded on an Ultraflex-II TOF/TOF mass spectrometer (Bruker Daltonic, Germany) equipped with MALDI source, nitrogen laser, LIFT cell for fragment-ion post-acceleration and gridless ion reflector. The software *Flex Control* 2.4, *Flex Analysis* 2.4 and *Biotools* 3.0 were used to operate the instrument and analyse the data. A peptide-calibration mixture (Bruker Daltonics, Germany) was used for external calibration.

2.4.2. N-terminal sequencing. Three large intergrown crystals from a 2 µl drop with 2 µg protein were fished out from the drop and washed in crystallization buffer before being dissolved in SDS loading buffer. Protein bands from the unstained SDS gel were blotted on a methanol-activated polyvinylidene fluoride membrane (PALL; Gelman Laboratory, USA) in 50 m*M* sodium borate, 20% methanol pH 9.0 buffer at 60 mA for 2 h. The membrane was stained in 0.006% Coomassie G250, 10% acetic acid and 30% methanol solution and air dried. The single protein band was excised and sent for N-terminal sequencing (Alphalyse Europe, Denmark).

2.4.3. Western blot. Reduced and nonreduced samples from the crystallization drop, as well as the starting material as a positive control, were loaded onto a denaturing SDS gel. Protein bands from the unstained SDS gel were blotted onto a nitrocellulose transfer

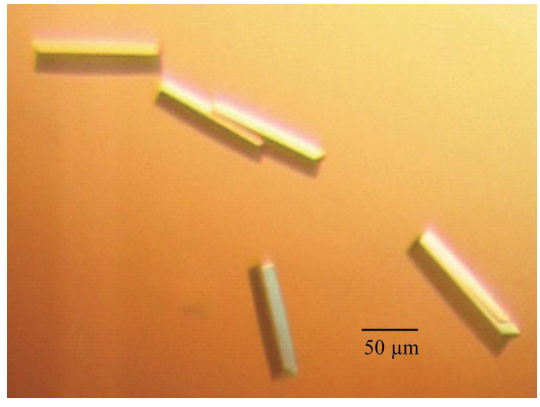

Figure 1
Crystals of Spz11.7 from 50 m*M* Tris–HCl, 20% PEG 3350 pH 8.0 with 10 m*M* betaine monohydrate as an additive.

membrane (BioRad Laboratories) at 60 mA for 2 h. The membrane was incubated in 1× PBS (10 m*M* sodium phosphate, 150 m*M* sodium chloride pH 7.2), 4%(*w*/*v*) milk powder, 0.2%(*v*/*v*) Tween-20 for 1.5 h before overnight application of the first antibody, mouse anti-His (Roche). After three washing steps with 1× PBS, 4% milk powder, 0.2% Tween-20, the second antibody, peroxidase-coupled goat anti-mouse (Chemicon International, USA), was applied for 4 h. The blot was treated with chemiluminescent reagents (Amersham Biosciences) after three washing steps in the absence of milk powder. His-tagged proteins were visualized after development and fixing (Kodak, Sigma–Aldrich) of the detection film (Roche).

3. Results and discussion

Initial crystals of the Spätzle isoform Spz11.7 appeared after three months and diffracted in-house to ∼7 Å resolution. These could be reproduced and improved using the crystallization additive betaine monohydrate (Fig. 1). The optimized crystals, which grew within three weeks, diffracted to 2.8 Å resolution. This large jump in resolution may be attributable to the presence of the additive, the larger volume of the crystals, their accelerated growth or a combination of these factors. The crystals belonged to the orthorhombic space group $P2_12_12_1$, with unit-cell parameters a = 53.0, b = 59.2, c = 62.5 Å (data-collection statistics are summarized in Table 1). As the unit-cell parameters and space group precluded the presence of a dimer of pro-Spätzle Spz11.7 (molecular weight 57 kDa) in the crystals, their contents were subjected to further analysis.

The starting material and dissolved crystals as well as selected negative crystallization experiments were analysed using denaturing SDS–PAGE. While the starting material yielded a major band corresponding to a molecular weight of 54 kDa (nonreducing conditions; 27 kDa under reducing conditions), analysis of the dissolved crystals revealed a fragment of ∼25 kDa (nonreduced samples, Fig. 2; ∼12 kDa under reducing conditions, data not shown). The crystals therefore contain a partially degraded disulfide-linked dimer of Spätzle. In order to identify this fragment, samples were subjected to mass spectrometry, N-terminal sequencing and Western blot analysis.

Protein bands excised from nonreducing denaturing SDS gels (Fig. 3) were subjected to MALDI-MS. The fingerprints of three samples of the same size as the crystallized fragment showed peptide masses corresponding to amino acids 139–143, 148–162, 193–204, 205–217 and 228–237 (summarized in Fig. 4). These peptides are all located within the C-terminal disulfide-knot domain; the missing peptides of the C-terminal domain are either those containing cysteines expected to be disulfide-linked or smaller than 500 Da. A low-molecular-weight degradation product that did not appear in the gel sample of the crystallized fragment (Fig. 3) was also measured as a negative control. The fingerprint corresponded to residues 10–25, 26–39, 40–54, 55–66, 71–77, 78–84, 110–123 and 148–162 (Fig. 4), which with the exception of peptide 148–162 are all located in the N-terminal propeptide of Spz11.7.

To identify the N-terminus of the crystallized fragment, which according to the MALDI-MS analysis could be anywhere between amino acids 123 and 139, N-terminal sequencing of washed and dissolved crystals was performed. Six cycles of Edman degradation yielded the sequence V/A-*X*-*X*-Y/S-D-E/Q with low signal strength and glycine contamination, which corresponds perfectly and uniquely to Spz11.7 residues ^{124}V-G-G-S-D-E^{129}. Thus, the N-terminus (which also corresponds to the N-terminus of mature Spätzle after activation

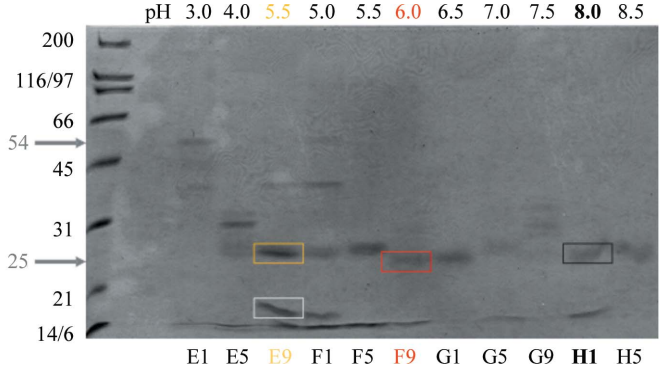

Figure 3
Nonreducing SDS–PAGE of Spz11.7 crystallization screening experiments using 4% PEG 3350 as precipitant and 0.05 *M* buffer. The pH values of individual crystallization drops are indicated and were achieved using the following buffers: sodium citrate (E1–F5), MES (F9), bis-tris–HCl (G1), imidazole–HCl (G5), sodium HEPES (G9) and Tris–HCl (H1–H5). Note the varying degradation bands observed. Lanes E9, F9 and H1 exhibit comparable bands (∼25 kDa) to those present in the crystals (see Fig. 2). Marked gel slices from E9, F9 and H1 were further analysed using MALDI-MS (see Fig. 4).

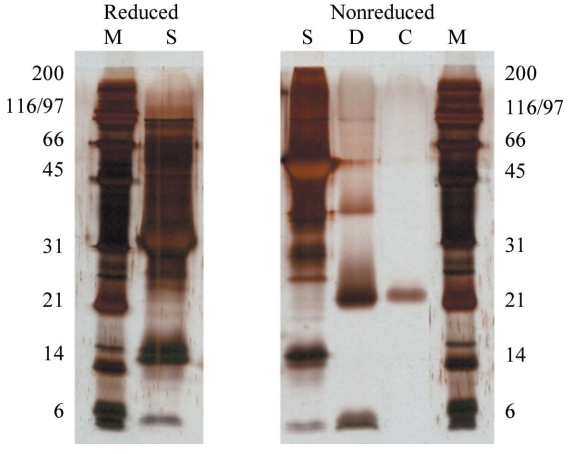

Figure 2
Silver-stained SDS–PAGE of Spz11.7 used for crystallization (lane S, starting material), a crystallization drop (lane D) and a dissolved crystal (lane C); Lane M, molecular-weight markers (kDa).

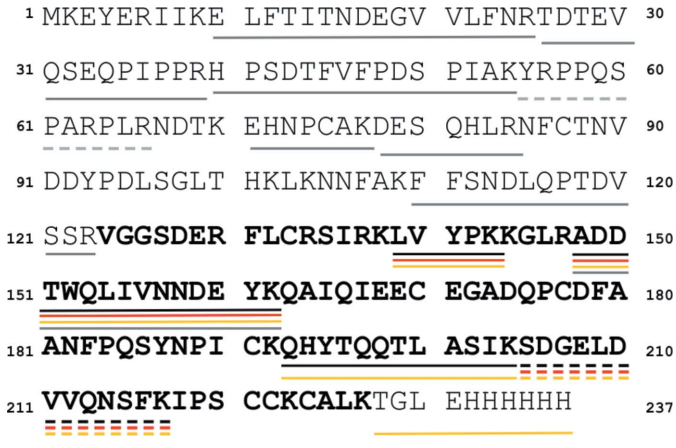

Figure 4
Recombinant Spz11.7 sequence, indicating the N-terminal propeptide as well as the mature cystine knot (bold). The peptides detected by MALDI-MS are underlined in black (from sample H1), red (sample F9), gold (sample E9, high-molecular-weight band) or grey (negative control, E9 low-molecular-weight band, see text for details). The dashed line indicates a peptide with ambiguous assignment (peptide mass ^{55}Y–R^{66}, 1437.807 Da; ^{205}S–K^{217}, 1437.686 Da).

cleavage) is in agreement with the MALDI-MS data, where the last non-included peptide is 110–123 and the first included peptide is 139–143. As the His_6 tag peptide 228–237 only occurred in one of three MALDI-MS samples, the presence of an intact C-terminus was examined by Western blotting against the C-terminal His_6 tag. As signals were obtained from both reduced and nonreduced samples of the starting material (positive control) but not from the crystallization drop sample (data not shown), the C-terminal His_6 tag of Spz11.7 does not appear to be present in the crystals.

Thus, the crystals contained the C-terminal cystine-knot-containing fragment Val124–Lys227. It is known that the propeptide of Spätzle isoforms is highly susceptible to trypsin cleavage (Weber *et al.*, 2003, 2005). The N- and C-termini of the crystallized fragment are consistent with a trypsin-like activity cleaving Spz11.7 after Arg123 and Lys227, although we have no clear evidence for such contamination. Based on the unit-cell parameters and molecular weight of mature Spätzle, the crystals are likely to contain a dimer in the asymmetric unit (Matthews coefficient V_M = 2.23 Å^3 Da^{-1}, corresponding to a solvent content of 45%; Matthews, 1968). A preliminary molecular-replacement search carried out using *Phaser* (McCoy *et al.*, 2005) with diverse NGF monomer and dimer structures as search models [PDB codes 1btg (Holland *et al.*, 1994), 1sg1 (He & Garcia, 2004), 1bet (McDonald *et al.*, 1991) and 1sgf (Bax *et al.*, 1997)] has so far failed to yield a satisfactory solution. A search for heavy-atom derivatives is under way, as are attempts to obtain crystals diffracting to higher resolution using synchrotron radiation.

This work was supported by the SFB610 'Protein-Zustände mit zellbiologischer und medizinischer Relevanz' and the Graduiertenkolleg 1026 'Conformational transitions in macromolecular interactions' of the DFG.

References

Bax, B., Blundell, T. L., Murray-Rust, J. & McDonald, N. Q. (1997). *Structure*, **5**, 1275–1285.
Bergner, A., Oganessyan, V., Muta, T., Iwanaga, S., Typke, D., Huber, R. & Bode, W. (1996). *EMBO J.* **15**, 6789–6797.
DeLotto, Y. & DeLotto, R. (1998). *Mech. Dev.* **72**, 141–148.
He, X. L. & Garcia, K. C. (2004). *Science*, **304**, 870–875.
Hoffmann, A., Funkner, A., Neumann, P., Walther, M., Weininger, U., Schierhorn, A., Balbach, J., Reuter, G. & Stubbs, M. T. (2008). Submitted.
Hoffmann, J. A. (2003). *Nature (London)*, **426**, 33–38.
Holland, D. R., Cousens, L. S., Meng, W. & Matthews, B. W. (1994). *J. Mol. Biol.*, **239**, 385–400.
Jang, I. H., Chosa, N., Kim, S.-H., Nam, H. J., Lemaitre, B., Ochiai, M., Kambris, Z., Brun, S., Hashimoto, C., Ashida, M., Brey, P. T. & Lee, W. J. (2006). *Dev. Cell*, **10**, 45–55.
Jin, M. S., Kim, S. E., Heo, J. Y., Lee, M. E., Kim, H. M., Paik, S. G., Lee, H. & Lee, J. O. (2007). *Cell*, **130**, 1071–1082.
Kabsch, W. (1993). *J. Appl. Cryst.* **26**, 795–800.
McCoy, A. J., Grosse-Kunstleve, R. W., Storoni, L. C. & Read, R. J. (2005). *Acta Cryst.* D**61**, 458–464.
McDonald, N. Q., Lapatto, R., Murray-Rust, J., Gunning, J., Wlodawer, A. & Blundell, T. L. (1991). *Nature (London)*, **354**, 411–414.
Matthews, B. W. (1968). *J. Mol. Biol.* **33**, 491–497.
Mizuguchi, K., Parker, J. S., Blundell, T. L. & Gay, N. (1998). *Trends Biochem. Sci.* **23**, 239–242.
Rudolph, R. & Lilie, H. (1996). *FASEB J.* **10**, 49–56.
Schneider, D. S., Jin, Y. S., Morisato, D. & Anderson, K. V. (1994). *Development*, **120**, 1243–1250.
Stein, D., Roth, S., Vogelsang, E. & Nusslein-Volhard, C. (1991). *Cell*, **65**, 725–735.
Weber, A. N. R., Gangloff, M., Moncrieffe, M. C., Hyvert, Y., Imler, J. L. & Gay, N. J. (2007). *J. Biol. Chem.* **282**, 13522–13531.
Weber, A. N. R., Moncrieffe, M. C., Gangloff, M., Imler, J. L. & Gay, N. J. (2005). *J. Biol. Chem.* **280**, 22793–22799.
Weber, A. N. R., Tauszig-Delamasure, S., Hoffmann, J. A., Lelievre, E., Gascan, H., Ray, K. P., Morse, M. A., Imler, J. L. & Gay, N. J. (2003). *Nature Immunol.* **4**, 794–800.